CONTRIBUTION OF SECONDARY SLIP SYSTEMS IN THE DEFORMATION PROCESS OF Ni MONOCRYSTALS*

By T. Uliasz

Department of Solid State Physics, Polish Academy of Sciences, Zabrze**

(Received June 16, 1976)

Both dislocation and mosaic structure of Ni-monocrystals deformed within the second stage of work-hardening with orientation favoring a multisystem slip have been investigated by X-ray and electron microscopy techniques. The effects of temperature and strain stresses on the activation of secondary slip systems have been analysed.

1. Introduction

The activity of slip systems under plastic deformation depends on the direction of the deforming force with respect to the crystallographic orientation. For plastic deformation of fcc monocrystals, extended along direction [100], four slip system act from the very beginning [1]. For crystals with middle orientation only one slip system is active at first. As the strain develops, secondary slip systems contribute to the deformation [2].

The work-hardening of the material is accompanied by a plastic deformation process. No uniform theory, even for crystals with middle orientation, has been developed so far [3, 4]. Investigations concerning the real structure of crystals with different deformation stages are of substantial importance for the development of the work-hardening theory. So far these studies have been carried out systematically only for fcc crystals with middle orientation. Those investigations concerned mainly the arrangement and structure of the slip lines [5, 6] and dislocation structure of the deformed crystals [7–11]. For crystals with an orientation favouring the multisystem slip that problem is actual.

The purpose of this investigation is to examine the contribution of secondary slip systems to the deformation process in Ni single crystals with orientations favouring a multisystem slip. Studies of the effects of both temperatre and strain stresses on the activation of secondary slip systems have been carried out.

---

* Supported by the Institute of Physics of the Polish Academy of Sciences.

** Address: Zakład Fizyki Ciała Stałego, Polska Akademia Nauk, Kawalca 3, 41-800 Zabrze, Poland.

2. Results and discussion

Monocrystals for work-hardening investigations were prepared in the shape of rods 12 mm in diameter and 60–80 mm long. All crystals were vacuum annealed for 24 hours at 1200°C. Chemical analysis has shown that the concentration of impurities does not exceed 0.1% with cobalt dominating.

Work-hardening curves have been found by means of the tensile test. The deformation rate was equal to about $10^{-4}s^{-1}$. Fig. 1 displays the work-hardening curves at various temperatures. The crystallographic orientation of a sample axis is shown in stereographic

TABLE I

Slip systems of samples of orientations [210 100 75], where the shear-stress $\tau = A\sigma$ has the highest value. σ — normal stress acting on the cross section of the sample

Slip system	A
primary $(11\bar{1})$ [101]	0.46
I secondary $(1\bar{1}1)$ [110]	0.39
II secondary (111) $[10\bar{1}]$	0.36

projection. This orientation distinguishes three slip systems. The shear stresses exerted in these systems have been listed in Table I. The value of a slip strain corresponding to the transition from the first to the second stage of work-hardening is distinctly smaller than that for crystals with similar purity but with an orientation that favours one slip system [12].

Both electron microscopy and the X-ray spectrometer with oscillating film techniques were utilised for the purpose of structural studies. By electron microscopy methods the dislocation structure in thin foils of {111} orientation have been investigated, these foils having been cut parallel to both the primary and secondary slip planes. In order to identify the dislocations, a contrast analysis in different {111} type reflexes were applied [8, 13].

The topography of a surface cut parallel to the primary slip system $(11\bar{1})$ and the shape of narrow interference stripes were taken off by means of the X-ray spectrometer with an oscillating film [14]. The estimated density of dislocations was deduced from measurements of the intensity distribution across the stripes. Information concerning the mosaic structure and the activity of secondary slip systems, however, were gained from topographic studies. Samples for both the X-ray and electron microsopy tests were cut with a spark machine, whereas further treatment was carried out by means of chemical and electrochemical polishing methods [15].

On the basis of X-ray and electron-microscopy investigations it has been found that structural changes caused by the influence of both temperature (in the case of less deformed samples) and the degree of deformation had taken place. For less deformed samples it was found that in foils cut parallel to the plane $(11\bar{1})$ the dislocations were grouped in concentration placed parallel to direction $[\bar{1}21]$, independently of the deformation temperature (Fig. 2). The distance from one concentration to the next was equal to 5 μm and

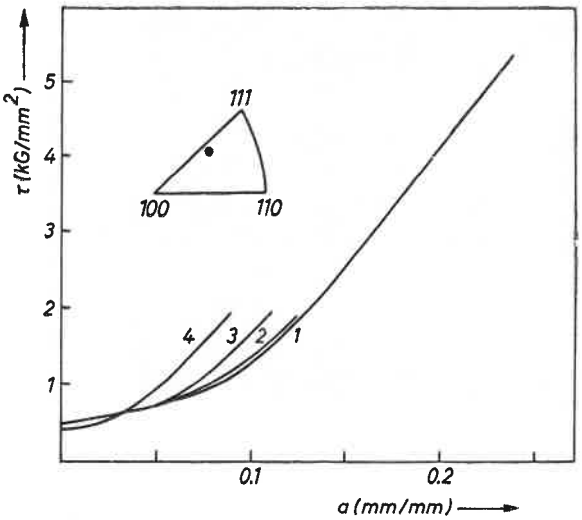

Fig. 1. Work-hardening curves of Ni monocrystals: *1* — strongly deformed sample at 200 K, *2, 3, 4* — weakly deformed samples at 200 K, 300 K, 400 K, respectively

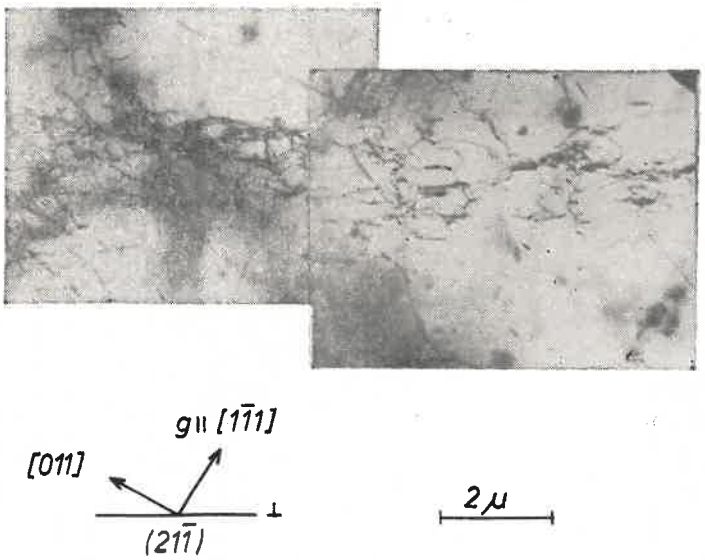

Fig. 2. Dislocation structure of a sample deformed at 400 K, (τ = 1.8 kG/mm²) in foil (11$\bar{1}$) within the reflex (1$\bar{1}$1). Within the concentration of dislocations extending in direction [$\bar{1}$21] the dislocation loops and dipoles are visible

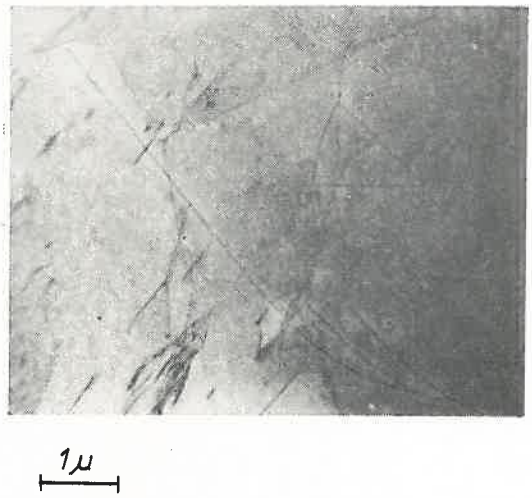

Fig. 3. Long dislocations spreading over the plane $(1\bar{1}1)$ of the secondary slip system, most often observed for samples deformed at high temperatures running through the concentration of short dislocation lines belonging to the primary system

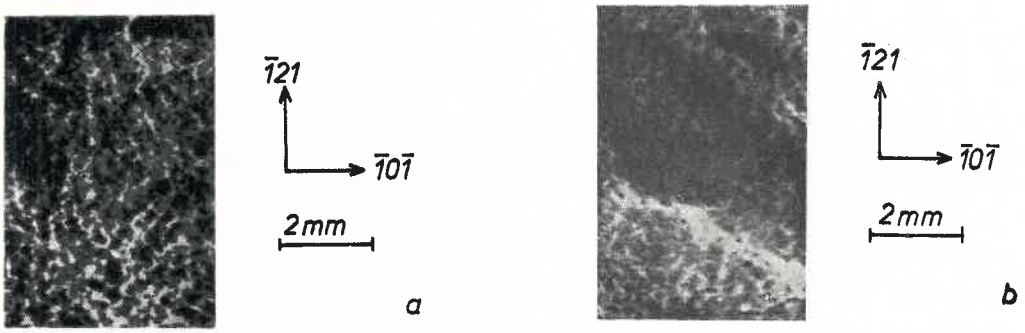

Fig. 4. Topographies of the surface $(11\bar{1})$ made within the reflex $(11\bar{1})$ for the following samples: a — (No 2), b — (No 4) deformed at 200 K and 400 K, respectively (τ = 1.8 kG/mm^2). The bands secondary slip are not visible

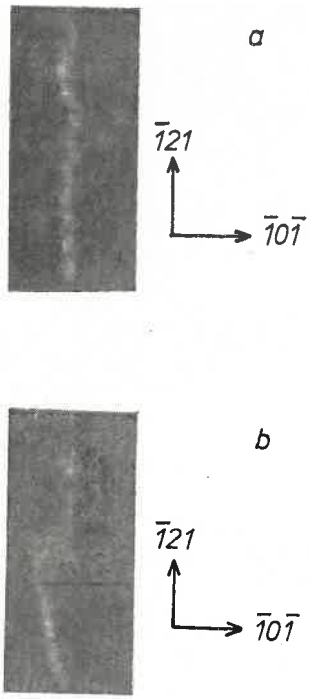

Fig. 5. Comparison of the shape of the interference stripes made within the reflex $(11\bar{1})$ for the samples: a, b — deformed at 200 K and 400 K respectively ($\tau = 1.8$ kG/mm^2)

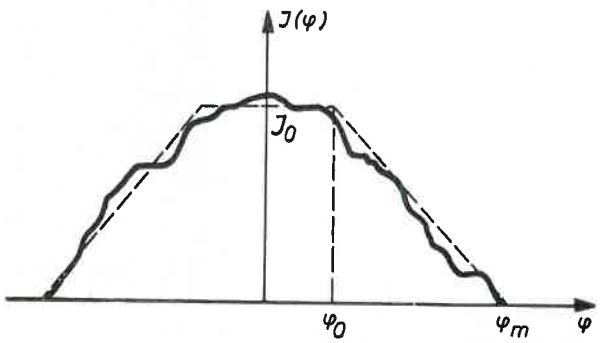

Fig. 6. The distribution of angular intensity of the interference stripes for weakly deformed samples. The dashed line presents a trapezium shaped distribution instead of that which was found experimentally

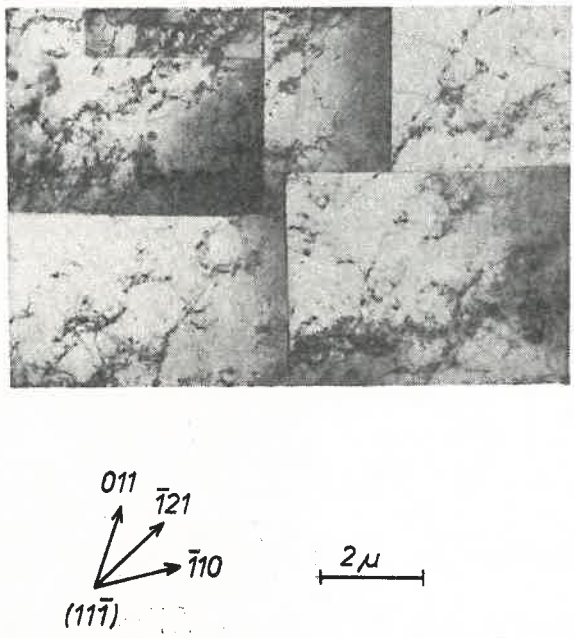

Fig. 7. Typical picture of the dislocation net observed in both $(11\bar{1})$ and $(1\bar{1}1)$ foils for a strongly deformed sample ($\tau = 5.3$ kG/mm²)

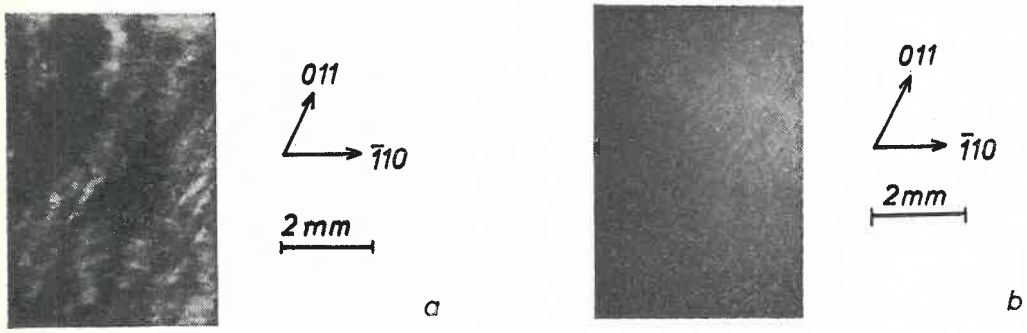

Fig. 8. Topographies of the surface $(11\bar{1})$ of a strongly deformed sample ($\tau = 5.3$ kG/mm²) made in the following reflexes: a — $(11\bar{1})$ and b — $(31\bar{1})$. Within the reflex of $(31\bar{1})$ and also in the reflex $(11\bar{1})$ the visible bands extended towards direction [011], resulting from the laminar arrangement of dislocations of the secondary slip system $(1\bar{1}1)$ [110]. Similar pictures have not been observed in weakly deformed samples

decreased slightly with an increase in the deformation temperature. Within the concentration the edge-type dislocations dominated. Differences in the dislocation structure of less deformed samples of the $(11\bar{1})$ foils concerned mainly the densities of both the loops and the dislocations dipoles of small geometrical sizes. The density increase of these components of the dislocation structure became evident when the deformation temperature increased.

Based on the structure pattern in foils cut parallel to plane $(1\bar{1}1)$ the activity of the $(1\bar{1}1)$ [110] secondary slip system may be evaluated. The dislocation density in foils cut from samples deformed at higher temperature was greater than in the case of foils from the samples deformed at 200 K (Fig. 3).

The X-ray surface topography (Fig. 4) displayed the mosaic structure more distinctly than in undeformed samples. An increase in the deformation temperature was accompanied by the appearance of macroblocks, which were distinctly registered in studies of narrow interference stripes (Fig. 5). Their presence was revealed by local bends in the stripes. The appearance of macroblocks may be associated with the increasing influence of secondary dislocations, whose different density in various regions of the sample might have contributed to local pilings of the primary dislocations.

In order to evaluate the density of dislocations generated in the process of deformation, attemps have been made to estimate the mean disorientation of mosaic blocks. For this purpose the distribution of the intensity of the narrow interference stripes had to be found by means of a microphotometer. During the exposure of the photographic plate the sample was arranged in such a way that the direction of the main spectrometer axis would cover direction $[\bar{1}21]$, which was parallel to the edge dislocation lines of the primary system. The oscillations of the samples within the range of $\pm 0.5°$ was accompanied by shift along the direction [101] at a distance of 1 mm. Thus it became possible to register the effect of the primary edge dislocations, which mainly decided the disorientation of the mosaic blocks.

The intensity distribution $J(\varphi)$, characteristic for the less deformed samples, has been presented in Fig. 6. Based on the found intensity distribution, it has been attempted to estimate the mean value of the angle φ, on which the other blocks are disoriented, relative to the most numerous blocks, i.e. those that had brought about the maximum intensity at $\varphi = 0$. Therefore the formula for the weighted average was applied. If function $N(\varphi)$ is treated as a function of the angular distribution of the blocks, which attributed to the disorientation range $[\varphi, \varphi + d\varphi]$, as many as $N(\varphi)d\varphi$ blocks, so the weighted average $\bar{\varphi}$ is expressed by the formula

$$\bar{\varphi} = N_0^{-1} \int_{-\infty}^{+\infty} \varphi N(\varphi) d\varphi. \tag{1}$$

The total number of blocks N_0 penetrated within the exposure time by an X-ray beam is equal to

$$N_0 = \int_{-\infty}^{+\infty} N(\varphi) d\varphi. \tag{2}$$

The value of $\bar{\varphi}$ was estimated with the following assumptions:
— the intensity J is proportional to the number of blocks N, disoriented by angle contained within the range $[\varphi, \varphi+d\varphi]$, i.e. $N(\varphi) = cJ(\varphi)$,
— the experimentally found intensity distribution $J(\varphi)$ can be replaced by a trapezium-shaped distribution, as shown in Fig. 6, for which

$$J(\varphi) = \begin{cases} J_0 & \text{for } 0 \leqslant \varphi \leqslant \varphi_0, \\ J_0\left(1 - \dfrac{\varphi-\varphi_0}{\varphi_m-\varphi_0}\right) & \text{for } \varphi_0 \leqslant \varphi \leqslant \varphi_m. \end{cases} \tag{3}$$

Then the weighted average of $\bar{\varphi}$, expressed by formula (1), can be expressed as

$$\bar{\varphi} = \pm\tfrac{1}{6}\left[(\varphi_0+\varphi_m) - \frac{\varphi_0\varphi_m}{\varphi_0+\varphi_m}\right]. \tag{4}$$

The possibility of changing the sign of the disorientation angle at the transition from one block to another has not been taken into consideration while deriving this formula. However, this is very probable for crystals deformed as a result of tension. The disorientation value $\bar{\varphi}$ calculated according to formula (4) would be, of course, too high for ideally bended crystals. However, in the case of crystals deformed as a result of tension, where φ_m has a restricted value which is independent of the value of the displacement of the crystal during exposure, the applied method of calculating the mean disorientation of the blocks can reflect reality well enough.

The mean increase in the disorientation $\Delta\bar{\varphi}$ of the blocks in the case of less deformed crystals, calculated by means of equation (4), was equal to about 12′. Assuming further, that the increase in the disorientation of the blocks as confirmed by investigations, of narrow stripes, is mainly due to edge dislocations, it is possible to calculate their densities. For the mean disorientation $\Delta\bar{\varphi}$, the linear density of dislocations on the block interfaces amounts to

$$N_l = \frac{\Delta\bar{\varphi}}{b}. \tag{5}$$

If the mean size of the blocks is α, there are $2\alpha N_l$ dislocation lines on each of the blocks. Then the area of a surface 1 cm^2 is covered by α^{-2} blocks. Thus the dislocation density N may be expressed as

$$N = 2N_l\alpha^{-1} \tag{6}$$

or

$$N = \frac{2\Delta\bar{\varphi}}{\alpha b}. \tag{7}$$

In the case of less deformed samples the dislocation density estimated on the basis of Eq. (7) amounts to about $N_s = 6\times10^8$ cm^{-2} and is independent of the deformation

temperature. The dislocation density of more deformed samples, evaluated by means of the method mentioned above, is equal to about $N_m = 5 \times 10^9$ cm^{-2}. The ratio of the dislocation densities N_m/N_s is equal to the ratio of the squares of shear stresses acting in the final stages of the work-hardening process of both less and more deformed samples;

$$\frac{\tau_m^2}{\tau_s^2} \approx \frac{N_m}{N_s} = 0.12.$$

The relation between the stress τ and the dislocation density N, valid for the second stage of the-hardening of crystals oriented favourably for a unisystem slip also holds for the investigated crystals.

A markedly deformed sample was characterized by its structure which was essentialy different from that of the less deformed ones. These differences were found both by X-ray and by electron microscopy methods. Regions with compressions at intervals of more than 2 μm from one another were very rare. Dislocations which make up a lattice belong to the primary and secondary slip systems. The pattern of the dislocation structure presented in (Fig. 7) is typical for both the $(11\bar{1})$ foils cut parallel to the primary system plane, and for the $(1\bar{1}1)$ foils cut parallel to the secondary slip system. The presence of secondary dislocations was also registered in the course of X-ray investigations. In the topographies of plane $(11\bar{1})$, set up within $(11\bar{1})$ and $(31\bar{1})$ reflexes (Figs 8a and 8b), their presence was manifested by bands of changing intensity. The direction in which the bands run as well as their more distinct contrast within the reflex of $(31\bar{1})$ indicate that they result from secondary dislocations (with the Burgers vectors $\bar{b} \parallel [110]$) arranged laminarly on the planes $(1\bar{1}1)$.

There was no evidence that the secondary system (111) $[10\bar{1}]$ is involved although the shear stress acting within this system was only slightly smaller than in the secondary system $(1\bar{1}1)$ [110].

3. Conclusions

1. The direction in which axial tension forces have been acting upon the deformed monocrystals of nikel exhibited three slip systems. Studies concerning the effect of temperature and deformation stresses upon both the primary and secondary slip systems have been carried out.

2. The work-hardening curves of investigated crystals are similar to that of crystals with an orientation that favours the one system-slip.

3. The value of a glide strain corresponding the transition from the first to the second work-hardening stage is smaller than for crystals with an orientation that favours the one system slip and decreases quite distinctly as the deformation temperature rises.

4. They X-ray surface topography has not supplied any evidence the activity of the secondary slip systems in the less deformed samples ($\tau = 1.8$ kG/mm^2). Electron microscopy studies, however displayed the presence of secondary dislocations. Their density rose with an increase in the deformation temperature.

5. In samples which were deformed at higher temperatures, the density of loops and dislocation dipoles showed that their share in the dislocation structure increases.

6. By means of the X-ray topography method, it has been found that the first of the secondary slip systems in the markedly deformed sample ($\tau = 5.3$ kG/mm^2) is activated. Electron miroscopy observations indicated a similarity of the dislocation lattice structures of both the primary and secondary slip systems.

7. Although the shear stress acting in this system was only slightly smaller than in the secondary system $(1\bar{1}1)$ [110], there was no evidence that the secondary system $(111)[10\bar{1}]$ is involved even in a more deformed sample.

8. It has been found that the empirical proportion $N \sim \tau_{II}^2$, for crystals with an orientation that is favourable to a one system-slip, holds true also for the crystals investigated.

I wish to thank Professor dr W. Żdanowicz for his encouragement and help. I also wish to thank Professor dr J. Auleytner for providing an opportunity to use the spectrometer with the oscillating film and for giving his consent to the X-ray investigations in the Institute of Physics of the Polish Academy of Sciences.

REFERENCES

[1] W. Vorbrugg, H. Ch. Goetting, Ch. Schwink, *Phys. Status Solidi* **4a**, 257 (1971).
[2] R. W. K. Honeycombe, *Plasticheskaya deformatsiya metallov*, Moskva 1972.
[3] A. Seeger, *Dislocations and Mechanical Properties of Crystals*, New York 1957.
[4] N. F. Mott, *Trans AIME* **218**, 962 (1960).
[5] S. Mader, A. Seeger, C. Leitz, *J. Appl. Phys.* **34**, 3368 (1963).
[6] E. N. Andrade, C. Da, D. A. Aboav, *Proc. R. Soc.* **A240**, 304 (1957).
[7] S. Mader, A. Seeger, H. M. Thieringer, *J. Appl. Phys.* **34**, 3376 (1963).
[8] U. Essmann, *Phys. Status Solidi* **12**, 707 (1965).
[9] H. Mughrabi, *Phil. Mag.* **23**, 897 (1971).
[10] U. Essmann, *Phys. Status Solidi* **12**, 723 ((1965).
[11] U. Essmann, *Phys. Status Solidi* **17**, 725 (1966).
[12] P. Haasen, *Phil. Mag.* **3**, 384 (1958).
[13] P. B. Hirsch et al., *Electron Microscopy of Thin Crystals*, London 1965.
[14] J. Auletner, *Rentgenowskie metody badania mozaiki i dyslokacji w kryształach*, Warszawa 1964 (in Polish).
[15] W. J. Tegart, *The Electrolytic and Chemical Polishing of Metals*, Pergamon Press 1959.